Wind Tunnel Evaluation of PAM II Pressure Ports

FIKRI ADNAN AKYÜZ

Atmospheric Science Department, University of Missouri-Columbia, Columbia, Missouri

HENRY LIU

Civil Engineering Department, University of Missouri-Columbia, Columbia, Missouri

TOM HORST

Atmospheric Technology Division, National Center for Atmospheric Research, Boulder, Colorado*

(Manuscript received 22 March 1990, in final form 9 October 1990)

ABSTRACT

The Portable Automated Mesonet II (PAM II) is a network of automated remote weather stations developed by the National Center for Atmospheric Research (NCAR) for measuring wind speed and direction, atmospheric pressure, temperature, humidity, and precipitation. The atmospheric pressure is measured with a pressure transducer connected to the central opening of a round disk—the pressure port. Wind tunnel tests were conducted to determine wind effects on the atmospheric pressure measured with this port. Three port designs were tested in the wind tunnel and their performances were compared. It was found that the two with symmetric edges performed the best at high wind speeds. The expected pressure errors were evaluated for normal PAM II operation and were generally found to be less than the rms error in the pressure transducers. For special circumstances where these pressure errors cannot be neglected, the wind tunnel data and the procedures discussed here can be used to make appropriate corrections if the horizontal and vertical components of the wind velocity at the height of the pressure port are measured. Results of this study should be of value to those who intend to use PAM II or other systems to make measurements in severe storms such as tornadoes, hurricanes, downbursts, or mountain downslope winds.

1. Introduction

PAM (Portable Automated Mesonet) is a network of computerized automated remote weather stations developed and used by the National Center for Atmospheric Research (NCAR) for measurement of the horizontal wind speed and direction, atmospheric pressure, temperature, humidity, and precipitation. The first generation of PAM (PAM I) was used to study thunderstorms, squall lines, tornadic storms, hailstorms (Fujita and Wakimoto 1982), severe downslope winds, air quality, wind shear, weather modification effectiveness, and fog during the period between 1976 and 1982 (Brock et al. 1986). A second-generation PAM (PAM II) was developed in 1981–82 and first deployed in 1983.

The main difference between PAM II and PAM I is that they operate with different communication systems. The PAM I remote stations communicated data by direct ultra-high-frequency (UHF) radio links to a 45-m high repeater, or relay station, in the field that transmitted the data to a base station. The remote stations were set up in line of sight and within 25 km of the repeater. The PAM II stations transmit data to one of the National Oceanic and Atmospheric Administration's (NOAA) Geostationary Operational Environmental Satellites (GOES), and these satellites serve as the repeater that relays data to the NCAR base station. Because the GOES satellites are orbiting at a height of 36 000 km, the remote stations can be placed at any distance apart that the experiment's logistics can support.

Brock et al. (1986) described and analyzed the PAM II system for providing surface mesoscale data for the research needs of the atmospheric science community. In both PAM I and II, the atmospheric pressure is measured by a pressure transducer connected to a *port* that consists of a horizontal disk having a center opening on the lower face of the disk to sense the "undisturbed" or "true" atmospheric pressure. Figure 1 is a schematic of the pressure port.

Corresponding author address: Dr. Thomas Horst, NCAR, P.O. Box 3000, Boulder, CO 80307.

* The National Center for Atmospheric Research is sponsored by the National Science Foundation.

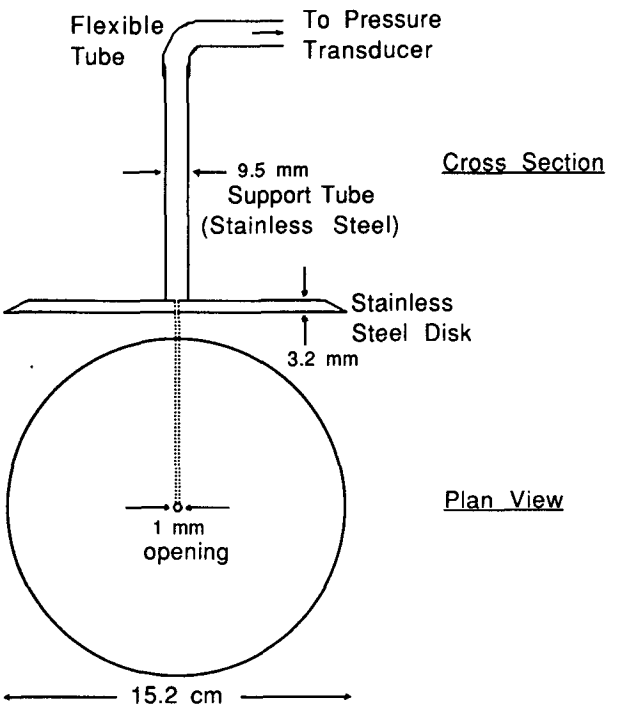

FIG. 1. PAM pressure port (asymmetric sharp edge).

Wind effect on the variation of pressure measured inside a building has been studied thoroughly in engineering literature in recent years (e.g., Liu 1991; Liu 1975). According to these studies, during high winds the barometer readings inside a building can be quite different from the undisturbed atmospheric surface pressure outside. The errors caused by wind can be determined as follows:

$$P_i - P_a = C_{p_i} \frac{\rho V^2}{2} \qquad (1)$$

where P_i is the pressure measured inside a building (i.e., the internal pressure); P_a is the ambient atmospheric pressure; ρ is the density of the air outside the building; V is the free-stream wind velocity at roof height; and C_{p_i} is the internal pressure coefficient—a dimensionless quantity that depends on the distribution of openings around the building.

The value of C_{p_i} for a building with uniform openings on different walls is of the order of -0.5 (Liu and Darkow 1988). Thus, Eq. (1) shows that at high wind speeds a large difference exists between atmospheric pressure and the pressure measured indoors. For example, at 30 m s^{-1} this difference is 230 Pa or 2.3 mb. Even though outdoor pressure measurements with PAM are unlikely to contain large errors, some errors caused by wind still exist at high speeds due to factors such as imperfect port design, imperfect mounting of the port, and existence of a vertical component of wind velocity. Consequently, an investigation of the wind effect on the pressure measured with PAM is still necessary.

A wind tunnel study has been conducted to determine whether the PAM II pressure port correctly senses the true or undisturbed atmospheric pressure under the influence of strong winds. The purpose of this paper is to report the result of this wind tunnel study, to analyze the magnitudes of wind-induced errors in the atmospheric pressure measured with PAM, and to explore ways to reduce such errors. Results of this study should be of value to those who plan to use PAM II to measure atmospheric pressure in high winds such as produced by tornadoes, hurricanes, downbursts associated with convective systems, and mountain downslope winds.

2. PAM II pressure port

The pressure measuring device in a PAM remote station consists of a pressure transducer, a circuit box (pressure transducer conditioner), and a port. The port consists of a horizontal stainless steel disk with a centrally located opening on its lower surface and a vertical support tube (see Fig. 1). The support tube and the disk are screwed together, leaving a flush surface on the bottom of the disk. The disk has a diameter of 15.2 cm, and the bottom opening has a diameter of 1 mm. The disk is mounted at a height of approximately 2 m above ground. The support tube of the port is connected to the pressure transducer through a flexible

tube or hose that runs from the top of the support tube, along a crossarm (boom) of the PAM tower, and down the mast to the circuit box, where it is connected to the pressure transducer.

3. Wind tunnel test

Although PAM remote stations are not subject to building internal pressure, they are influenced by a similar wind effect, especially if the wind is not parallel to the pressure port disk. This effect was assessed in a wind tunnel test using three pressure port designs. These designs differ only in the geometry of the disk: sharp asymmetric edge, sharp symmetric edge, and round symmetric edge (see Fig. 2). The tests were carried out in the civil engineering wind tunnel, University of Missouri–Columbia. The tunnel is of the aerodynamic type having a wind flow of uniform velocity profile and low turbulence intensity ($[\overline{u'^2}]^{1/2}/V$ less than 1%). The dimensions of the test sections are 91 cm × 91 cm. Such a flow provides a quasi-steady simulation of the instantaneous response of a PAM port in a turbulent wind with integral length scale or mean eddy size much larger than the diameter of the disk. The wind speed was measured with a Pitot tube mounted 45 cm (approximately) upstream of the disk at the disk height. The port was mounted in the center of the wind tunnel and tested at various tilt angles, α.

Two wind speeds were used for the wind tunnel tests: 12 and 28 m s^{-1}. The use of two different speeds allowed a check of any possible Reynolds number effect. The ambient pressure was measured by a wall tap on the wind tunnel wall of the test section. The pressure was measured with both a micromanometer and a differential pressure transducer (Valedyne model CD223). Flexible plastic tubing was used to connect the port to the pressure side of the micromanometer and the pressure transducer. Similar tubing connected the ambient pressure to the other end of the micromanometer and the pressure transducer. The disk was tilted for angles of attack α between +30° and −30°. Positive angles ($\alpha > 0$) occur when the bottom surface of the disk faces upstream, and negative angles ($\alpha < 0$) occur when the bottom of the disk faces downstream (see Fig. 2).

Each set of tests was conducted at a constant velocity, either 12 or 28 m s^{-1}. The velocity measurements were accurate within 2%, approximately. The angle of attack, α, was set prior to each test by a circular protractor equipped with a level. The accuracy of the angle measured was within 0.25°. Pressure readings were repeated three times for all the runs. Each of the data points in Figs. 3–6 represents the average of the three readings. The standard deviation of the three readings in each set is generally between 1% and 10% of the mean pressure, with larger percent errors for smaller pressures.

4. Test results

Tests were conducted at about ten angles of attack between plus and minus 30°. Angles beyond ±30° were not tested because it is very unlikely that a PAM remote station would encounter winds with such large angles of attack. The test results are presented in terms of the pressure coefficient C_p defined as follows:

$$C_p = \frac{P - P_a}{(1/2)\rho V^2} \tag{2}$$

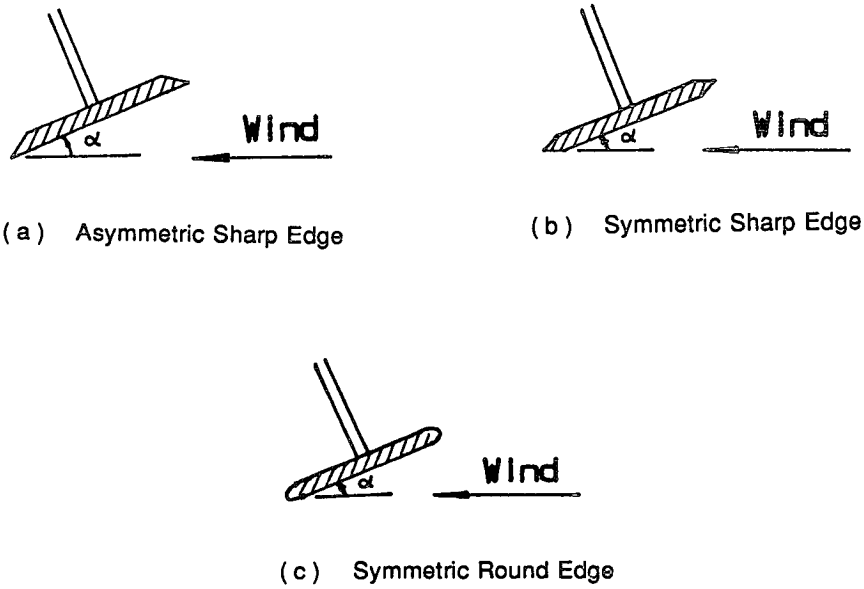

(a) Asymmetric Sharp Edge

(b) Symmetric Sharp Edge

(c) Symmetric Round Edge

FIG. 2. Three pressure port designs tested in wind tunnel. (Note that the angle of attack α is considered positive when the disks are tilted toward the wind as shown in this figure.)

where P is the pressure measured by the PAM pressure transducer; P_a is the ambient pressure; ρ is air density; and V is the wind speed at the disk height.

Figures 3, 4, and 5 give the test results for the three different port designs: asymmetric sharp-edged disk, symmetric sharp-edged disk, and symmetric round-edged disk. Each figure contains two graphs corresponding to the two velocities tested. Some common features of the three figures are:

(i) At $\alpha = 0°$, the value of C_p is negative—of the order of -0.1 depending on port design.

(ii) $C_p = 0$ at $\alpha \approx 5°$. Thus no error is generated in wind pressure measurements when $\alpha \approx 5°$.

(iii) C_p is positive for $\alpha > 5°$, and negative for $\alpha < 5°$.

(iv) A sudden change of slope of the curves occurs at $\alpha \approx -10°$; the value of C_p decreases rapidly for $\alpha < -10°$.

(v) The values of C_p are almost identical for the two velocities tested, 12 and 28 m s^{-1}. The values of C_p are expected to be insensitive to wind speed or to the port Reynolds number over a much wider range of wind speeds than tested here. Due to limitations of wind tunnel speed and the sensitivity of pressure sensors, the tests were not carried out beyond the present test range.

(vi) The absolute values of C_p are considerably greater for negative α than for positive α. This is caused by the pressure port inlet being in the wake generated by the disk at negative α.

In spite of the common features of the results based on the three designs, there are notable differences between the response of the current PAM II asymmetric sharp-edged disk and the two symmetric edge disks. At 12 m s^{-1}, the current PAM II design has better response near zero angle of attack than the symmetric-edge designs. It has a C_p at $\alpha = 0$ that is significantly smaller than for the symmetric-edge designs and, correspondingly, the angle at which $C_p = 0$ is $\approx 2°$ rather than $\approx 5°$. However, the asymmetric sharp-edged disk gave significantly higher negative values of C_p for values of α in the range $-10°$ to $-30°$. This can be seen more clearly from Fig. 6, which summarizes the results of the three designs at $V = 28$ m s^{-1}. For instance, at $\alpha = -15°$, while the two symmetric edge designs (round and sharp) give about the same value of $C_p = -0.4$, the asymmetric disk gives approximately $C_p = -0.8$, which is twice as large. Thus the current PAM II design produces less dynamic pressure error than the symmetric-edge designs at low wind speeds and small angles of attack and more dynamic pressure error in the range $-10°$ to $-30°$. (A final consideration when designing pressure ports is that a round-edged disk is safer and easier to maintain.)

5. Consequences for PAM II pressure measurements

A realistic assessment of the expected error in PAM II atmospheric pressure measurements over some averaging interval requires estimates for the probability

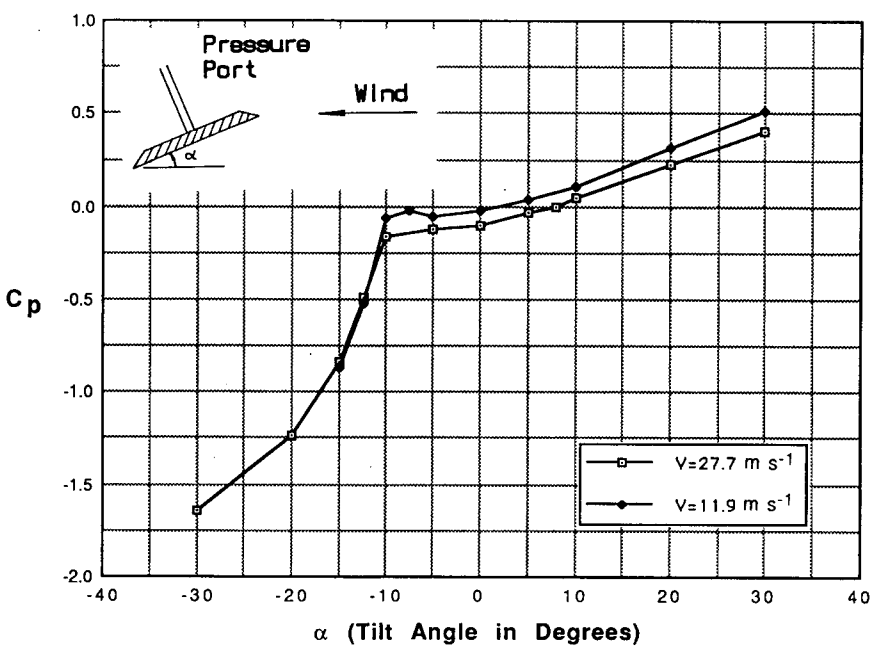

FIG. 3. Variation of pressure coefficient with tilt angle for nonsymmetric, sharp-edged port.

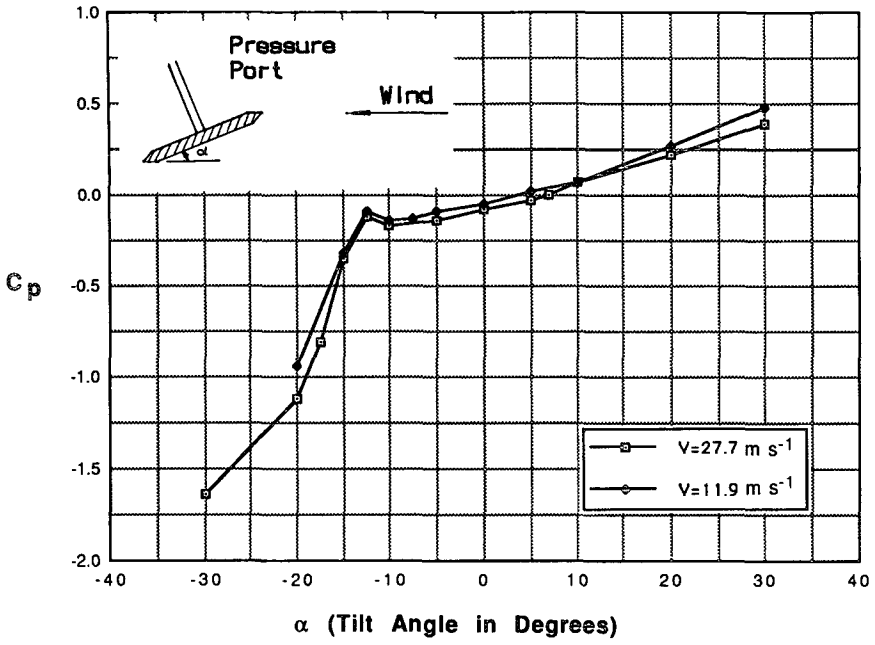

FIG. 4. Variation of pressure coefficient with tilt angle for symmetric, sharp-edged port.

distributions of both vertical and horizontal winds at the height of the pressure port, approximately 2 m above ground. Because the flow at this height is nearly always turbulent, these probability distributions should account for the fluctuations in the individual wind components. However, since the pressure errors increase with V^2 and are significant only at high wind speeds, fluctuations in the horizontal wind speed can be assumed negligible compared to fluctuations in the vertical wind component when calculating the angle of attack. For the same reasons, the atmospheric surface layer can be assumed to be neutrally stratified. If the mean angle of attack $\bar{\alpha}$ is zero, the (instantaneous) angle of attack is

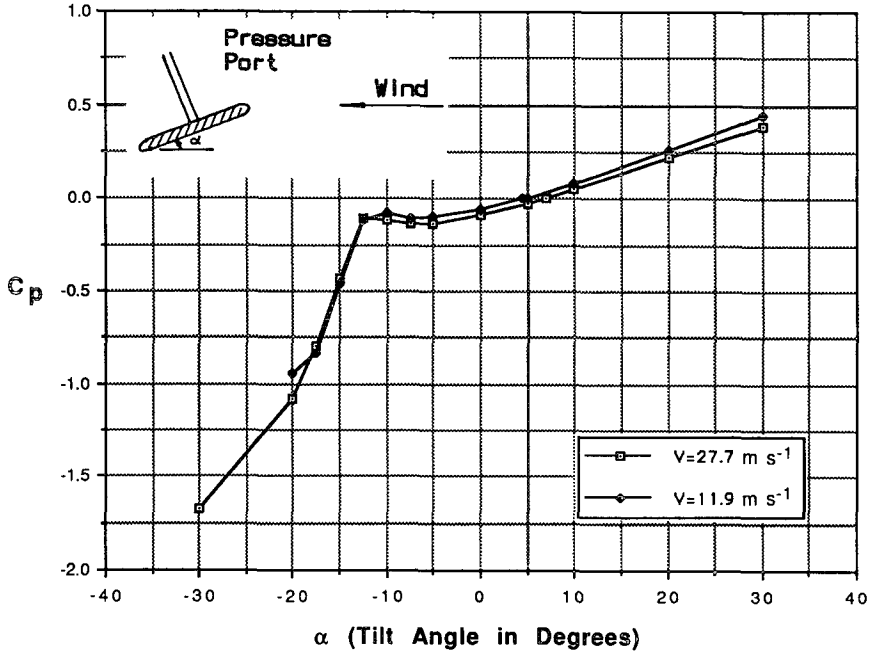

FIG. 5. Variation of pressure coefficient with tilt angle for symmetric, round-edged port.

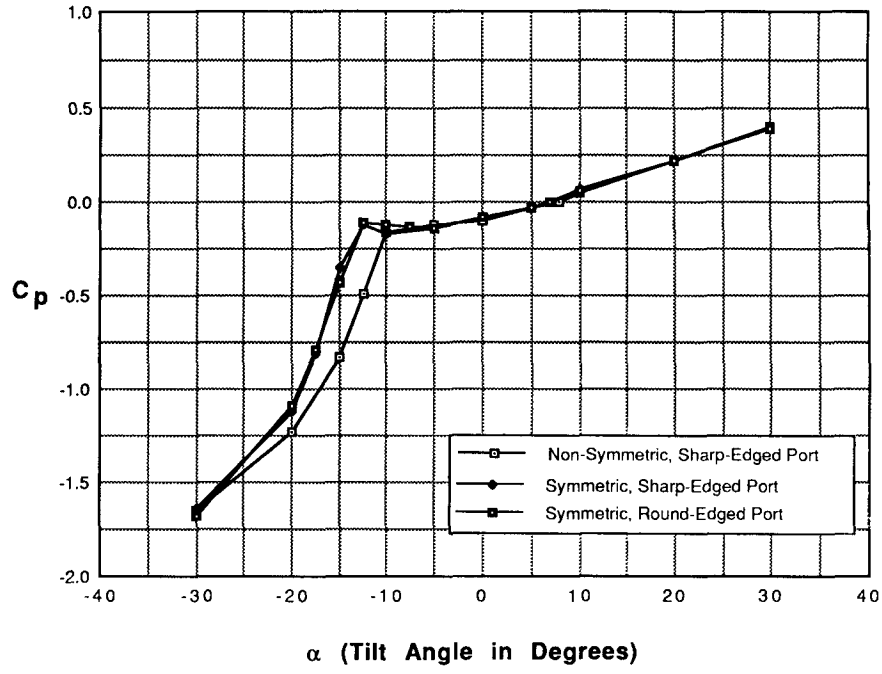

FIG. 6. Comparison of pressure coefficient for three different port designs (V = 27.7 m s^{-1}).

$$\alpha' = \arctan(w'/V) \tag{3}$$

$$= \arctan\left[\frac{w'}{\sigma_w}\frac{\sigma_w}{(u_*/k)\ln(z/z_0)}\right] \tag{4}$$

$$= \arctan\left[\frac{\sigma_w}{u_*}\frac{ky}{\ln(z/z_0)}\right]. \tag{5}$$

Here w' is the (instantaneous) vertical wind component; σ_w is the rms of w'; V is the mean horizontal wind speed; u_* is the surface friction velocity; k (=0.4) is the von Kármán constant; z is the measurement height; and z_0 is the surface roughness. Note that we have used the logarithmic wind profile $V = (u_*/k) \times \ln(z/z_0)$ applicable for neutral stratification. For neutral stratification, it is also known that $(\sigma_w/u_*) \approx 1.3$ (e.g., Wyngaard et al. 1974), and it can be assumed that $y = (w'/\sigma_w)$ is normally distributed.[1] Thus the expected value of C_p is only a function of z/z_0,

$$\langle C_p \rangle = \frac{1}{\sqrt{2\pi}}\int_{-\infty}^{\infty} C_p(\alpha)\exp\left(-\frac{y^2}{2}\right)dy. \tag{6}$$

In the majority of cases, $\bar{\alpha} = 0$ and $\alpha = \bar{\alpha} + \alpha' = \alpha'$. However, $\langle C_p \rangle$ has also been calculated for $-30° \leq \bar{\alpha} \leq +30°$. Since PAM II stations are deployed with the pressure port disk oriented horizontally, nonzero $\bar{\alpha}$ would correspond in most cases to a station location on sloped terrain. Figure 7 shows the expected pressure errors for the existing (nonsymmetric) PAM II pressure port, calculated from Eq. (2) for a mean wind speed of 10 m s^{-1} at a height of 2 m and for a range of surface roughness. The figure also lists the value of σ_α (rms of α) corresponding to each value of z/z_0. The case $z_0 = 0$, $\sigma_\alpha = 0$ corresponds to no vertical wind fluctuations and follows directly from the C_p data in Fig. 3 for V = 11.9 m s^{-1}. Because of the nonlinear dependence of C_p on angle of attack, the expected pressure errors for a realistic distribution of vertical wind fluctuations are markedly different from those for $\sigma_\alpha = 0$, particularly for $-15° \leq \bar{\alpha} \leq 0°$.

The expected pressure errors shown in Fig. 7 for a mean wind speed of 10 m s^{-1} must be adjusted for the expected climatological distribution of mean wind speeds at a height of 2 m. The wind speed distributions at many locations in the contiguous United States have been found to be reasonably approximated by a Weibull distribution with a shape factor of 2 (Justus et al. 1976), also known as the Rayleigh distribution:

$$F(V) = \frac{2V}{c^2}\exp\left[-\left(\frac{V}{c}\right)^2\right] \tag{7}$$

where $c = 2\langle V \rangle/\sqrt{\pi}$ is a function of the annual average wind speed $\langle V \rangle$. For many locations in the central United States, $\langle V \rangle$ at a height of 10 m is on the order of 5–6 m s^{-1}. Assuming a logarithmic wind profile and

[1] Calculations have also been made with a skewed distribution for the vertical wind component, as occurs in convective conditions. The results do not differ significantly from those for a normal distribution.

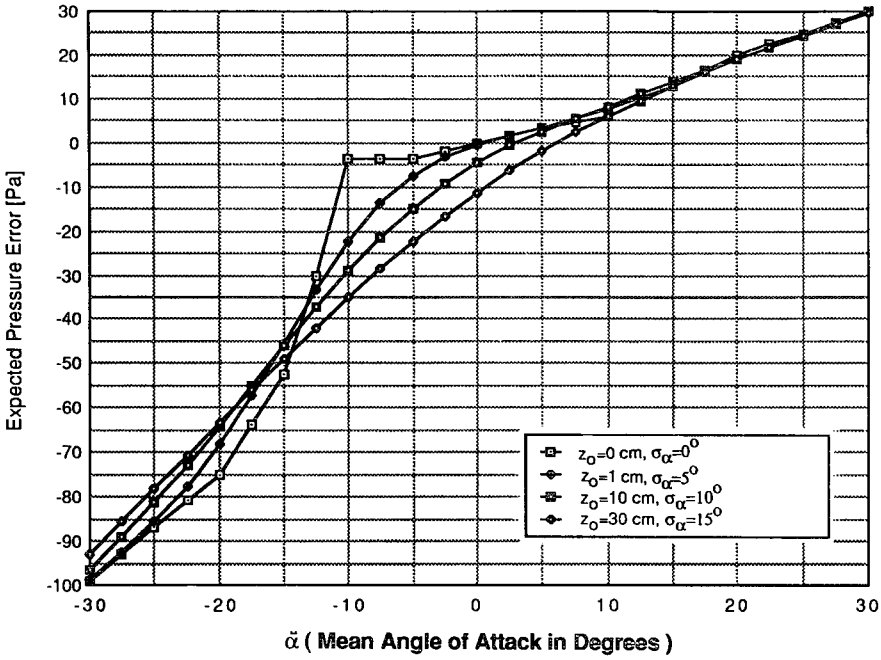

FIG. 7. Expected error for PAM II pressure port (nonsymmetric, sharp-edged port) at $V = 10$ m s^{-1} (1 mb = 100 Pa).

z_0 in the range of 1–10 cm, this implies $\langle V \rangle \approx 4$ m s^{-1} at 2 m. For a Rayleigh distribution with $\langle V \rangle \approx 4$ m s^{-1}, the wind speed is expected to exceed 10 m s^{-1} less than 1% of the time. In addition, the expected value of V^2 predicted from Eq. (7) is 20 m^2 s^{-2} and thus, since the pressure errors are scaled by the square of the wind speed, the errors are on average only 20% of those shown in Fig. 7.

Finally, these results should be compared with the measurement characteristics of the PAM II pressure sensor. Although the resolution of the pressure sensor is 2 Pa (0.02 mb), the rms error over the entire range of 60 to 110 kPa (600 to 1100 mb) is 40 Pa or 0.4 mb (Brock et al. 1986). Thus, under most circumstances the pressure error introduced by wind flow over the pressure port can be neglected. Special circumstances where this might not be the case are strong vertical wind gusts, such as microbursts associated with convective systems, in hurricanes, or in the measurement of local pressure gradients over complex terrain. These need to be treated on a case-by-case basis. If the three components of the wind velocity are measured near the location of the pressure port, the pressure data can be corrected by using Eq. (2) and the wind tunnel test data given in Figs. 3–6. However, normal PAM II measurements only include the horizontal wind components at a height of 10 m. That wind data could be used to estimate a correction for the time-averaged pressure as in the preceding analysis (Fig. 7) by estimating z_0 for the site and using the logarithmic wind profile to extrapolate the 10-m wind to the 2-m height of the pressure port. Over nonhorizontal terrain, $\bar{\alpha}$ could be estimated from the 10-m wind direction by assuming that the mean wind was parallel to the surface. Research is planned to demonstrate the ability to use PAM II to make such corrections in the field.

6. Conclusion

Wind tunnel measurements have been made of the dynamic pressure error caused by flow past PAM II pressure port disks. The wind-induced error is proportional to a pressure coefficient C_p, and it increases with the square of the wind speed [Eq. (2)]. For all three pressure port disk designs, the error is zero at an angle of attack of approximately 5°, and when the wind is parallel to the disks (i.e., zero angle of attack) a negative pressure coefficient is generated. At high wind speeds this coefficient is approximately −0.08 for all three disk designs, but at low wind speeds the asymmetric-edged disk has a significantly smaller coefficient on the order of −0.02. Increasingly larger negative C_p occurs for increasing negative angles of attack, and increasingly positive C_p occurs for increasing positive angles of attack.

The dependence of C_p on angle of attack is nonlinear. The pressure errors are noticeably greater when the pressure port inlet is on the lee side of the disk; i.e., in the wake of the flow past the disk, than when it is on the windward side. Thus, when the disk is horizontal,

larger pressure errors occur with a negative (downward) vertical wind component. The (negative) angle of attack at which the pressure error is magnified is larger with a symmetric-edged disk than with an asymmetric-edged disk. Thus, for negative angles of attack, symmetric edged disks have smaller pressure errors.

The wind-induced pressure errors expected for normal PAM II operation are less than the rms error in the pressure transducers except when high winds are encountered. For special circumstances where these pressure errors cannot be neglected, the wind tunnel data and the procedures discussed here can be used to correct the pressure data.

Acknowledgments. The authors are grateful for the capable assistance of Mr. Gerry Albright, NCAR, in completing this research.

REFERENCES

Brock, F. V., G. H. Saum and S. R. Semmer, 1986: Portable automated mesonet II. *J. Atmos. and Oceanic Technol.*, **4,** 573–582.

Fujita, T. T., and R. M. Wakimoto, 1982: Effects of miso- and mesoscale obstruction on PAM winds obtained during project NIMROD. *J. Appl. Meteor.*, **21,** 840–858.

Justus, C. G., W. R. Hargraves and A. Mikhail, 1976: Reference wind speed distributions and height profiles for wind turbine design and performance evaluation applications. ERDA ORO/5108-76/4, National Technical Information Service, Springfield, Virginia, 52 pp.

Liu, H., 1975: Wind pressure inside buildings. *Proc. of the 2nd U.S. National Conference on Wind Engineering Research,* Fort Collins, CO.

——, 1991: *Wind Engineering: A Handbook for Structural Engineers,* Prentice Hall, 209 pp.

——, and G. L. Darkow, 1988: Wind effect on measured atmospheric pressure. *J. Oceanic and Atmos. Technol.*, **1,** 6–12.

Wyngaard, J. C., O. R. Cote and K. S. Rao, 1974: Modeling the atmospheric boundary layer. *Adv. Geophys.*, **18A,** 193–211.